

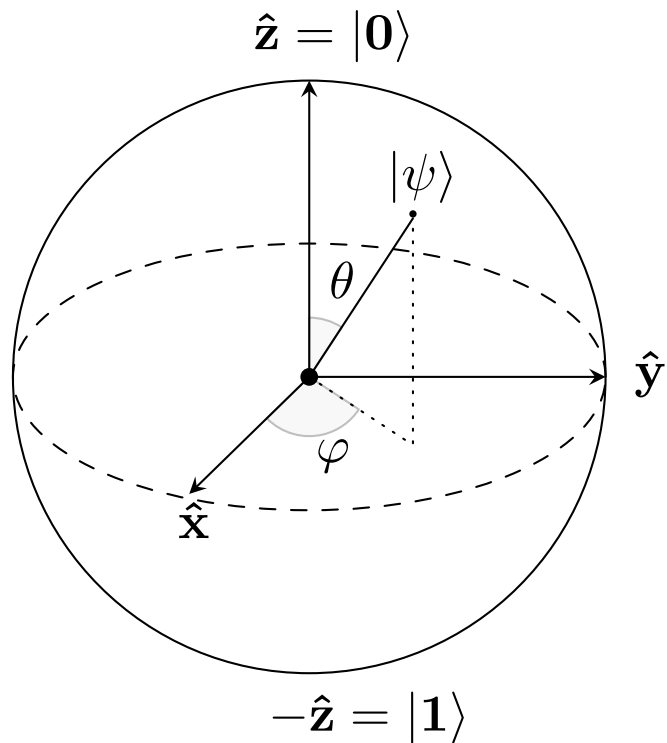


Report intership - 4A  
Polytech Clermont-Ferrand - GP4A (2023 - 2024)  
Engineering Physics Department

---

## Entanglement in a spin chain

---



**Vincent MARAIS**

Period: from 08/04/2024 to 22/08/2024

USACH, Av. Libertador Bernardo O'Higgins, 9170022 Estación Central, Región Metropolitana

USACH supervisor: Guillermo Romero

Polytech supervisor: Pascal Lafon

# **Abstract**

This study investigates the entanglement properties of a 1D lattice modeled by the Heisenberg XY model with the inclusion of Dzyaloshinskii-Moriya interaction (DMI). We analyze the concurrence between qubits under various configurations of the DMI constant  $D$ , the anisotropy parameter  $\delta$ , and the correction factor  $\gamma$ . Both 2-qubit and 3-qubit systems are considered to understand the influence of these parameters on quantum entanglement. Our findings reveal that the DMI generally enhances the entanglement between qubits, as indicated by increased concurrence values. However, the anisotropy parameter  $\delta$  introduces a competing effect that can reduce entanglement, particularly when  $\delta$  is increased. The results provide insight into how these parameters can be tuned to control entanglement in quantum systems, which is crucial for applications in quantum information processing and the design of quantum materials.

**Keywords :** Entanglement, Dzyaloshinskii-Moriya interaction, Heisenberg XY model

# Acknowledgements

I would like to begin by expressing my deep gratitude to Guillermo Romero, my tutor, Associate Professor in the Physics Department at the Universidad de Santiago de Chile, and researcher at the Center for the Development of Nanoscience and Nanotechnology (CEDENNA), for giving me such a warm welcome to Chile. I am extremely thankful for his support and for providing me with the opportunity to enjoy this unforgettable experience, which combined fascinating research with the discovery of Chile.

I would also like to extend my thanks to my academic tutor, Pascal Lafon, for his supervision and support.

Finally, I wish to acknowledge my family and all the people I met in Chile.



<b>List of Figures</b>	<b>IV</b>
<b>Introduction</b>	<b>1</b>
<b>1 Theoretical fundamentals</b>	<b>2</b>
1.1 Quantification of the Entanglement State . . . . .	2
1.2 Heisenberg XY model with DM interaction . . . . .	3
<b>2 Methodology</b>	<b>4</b>
2.1 Numerical approach . . . . .	4
<b>3 Results And Discussion</b>	<b>7</b>
3.1 Entanglement in a spin chain with 2 qubits . . . . .	7
3.2 Discussion . . . . .	8
3.3 Entanglement in a spin chain with N qubits . . . . .	10
<b>Conclusion</b>	<b>14</b>
<b>References</b>	<b>15</b>

## List of Figures

1	Schematic of the lattice of $L + 1$ qubits with the Heisenberg XY model and DMI, where the blue arrows represent the spin states of the qubits, and the gray waves represent the interaction between two neighboring qubits. . . . .	3
2	Schematic of the Proposition 7 . . . . .	4
3	Problem of calculation of the concurrence for many qubits . . . . .	6
4	$D = 0$ , Mean Squared Error: 1.51e-07, $\gamma = -1$ , $\delta = 1$ , $g = 1$ , $J = 1$ . . . . .	7
5	$D = 1$ , Mean Squared Error: 1.51e-07, $\gamma = -1$ , $\delta = 1$ , $g = 1$ , $J = 1$ . . . . .	8
6	Concurrence for different values of $D$ and $\delta$ with $\gamma = 1$ . The concurrence values indicate the level of entanglement in the qubit system over time, showing how different parameters influence the entanglement. . . . .	11
7	Concurrence for different values of $D$ and $\delta$ with $\gamma = 1$ in a 6-qubit system. The plots illustrate how these parameters affect the entanglement within the system over time. . . . .	12

# Introduction

Quantum entanglement, a fundamental feature of quantum mechanics, was first recognized in the early 20th century by Einstein, Podolsky, Rosen, and Schrödinger [5]. This phenomenon describes a situation where the quantum states of two or more particles become intertwined, such that the state of one particle cannot be described independently of the state of the other, no matter the distance separating them.

Entanglement becomes a practical resource in quantum information science, underpinning technologies such as quantum cryptography [7], quantum teleportation [1], and quantum computing [9]. These applications exploit entanglement to perform tasks that are impossible with classical systems.

Despite its utility, entanglement is a fragile and complex phenomenon, challenging to detect and manipulate. The study of entanglement involves understanding its properties, methods for its detection, and strategies for its quantification and manipulation. These efforts are crucial for advancing our ability to harness entanglement for practical applications, ensuring that it can be effectively used as a resource in quantum communication and computation.

The work presented a quantum simulation of a specific model of 1D lattice of **qubits** (quantum bit) a quantum system capable of existing in two states, such as the spin-up  $|\uparrow\rangle$  and spin-down  $|\downarrow\rangle$  states of an electron call Heisenberg XY model [8] and with a Dzyaloshinskii-Moriya interaction (DMI) [6, 4]. Finally a protocol to accelerating the entanglement in this lattice.

# 1. Theoretical fundamentals

In this section, we will discuss how to quantify entanglement in a quantum system. Finally we will express the Heisenberg XY model and the Dzyaloshinskii-Moriya interaction (DMI).

## 1.1 Quantification of the Entanglement State

Quantifying entanglement is crucial for evaluating the strength and practical applicability of quantum states. Among the various metrics, **concurrence** [10] is a widely used measure, especially in two-qubit systems. This section outlines the calculation of concurrence, which provides a numerical indicator of the degree of entanglement in a two-qubit quantum state. Concurrence  $C(\rho)$  is defined as:

$$C(\rho) = \max (0, \lambda_1 - \lambda_2 - \lambda_3 - \lambda_4) \quad (1)$$

Here,  $\lambda_i$  (for  $i = 1, 2, 3, 4$ ) are the square roots of the eigenvalues of the matrix  $\rho\tilde{\rho}$ , listed in descending order. The density matrix is defined as  $\rho = |\psi\rangle\langle\psi|$ , where  $|\psi\rangle$  represents the state of the two qubits. The matrix  $\tilde{\rho}$  is given by:

$$\tilde{\rho} = (\sigma^y \otimes \sigma^y) \rho^* (\sigma^y \otimes \sigma^y)$$

where  $\rho^*$  is the complex conjugate of  $\rho$ ,  $\otimes$  tensor product and  $\sigma^y$  is the Pauli-Y matrix:

$$\sigma^y = \begin{pmatrix} 0 & -i \\ i & 0 \end{pmatrix}$$

Concurrence values range from 0 to 1, where 0 denotes a separable (non-entangled) state, and 1 indicates a maximally entangled state. In two-qubit systems, the most recognized maximally entangled states are the Bell states:

$$\begin{aligned} |\Phi^+\rangle &= \frac{1}{\sqrt{2}} (|\downarrow\downarrow\rangle + |\uparrow\uparrow\rangle) \\ |\Phi^-\rangle &= \frac{1}{\sqrt{2}} (|\downarrow\downarrow\rangle - |\uparrow\uparrow\rangle) \\ |\Psi^+\rangle &= \frac{1}{\sqrt{2}} (|\downarrow\uparrow\rangle + |\uparrow\downarrow\rangle) \\ |\Psi^-\rangle &= \frac{1}{\sqrt{2}} (|\downarrow\uparrow\rangle - |\uparrow\downarrow\rangle) \end{aligned}$$

## 1.2 Heisenberg XY model with DM interaction

The Heisenberg XY model, can be described by the following Hamiltonian :

$$\hat{\mathcal{H}}_{XY} = J\hbar \sum_{n=1}^L \left[ \left( \frac{1+\delta}{2} \right) \sigma_n^x \otimes \sigma_{n+1}^x + \left( \frac{1-\delta}{2} \right) \sigma_n^y \otimes \sigma_{n+1}^y \right] + g\hbar \sum_{n=1}^{L+1} \sigma_n^z, \quad (2)$$

here,  $\hat{\sigma}_n^x$ ,  $\hat{\sigma}_n^y$ , and  $\hat{\sigma}_n^z$  are the Pauli matrices of the qubit  $n$  in the lattice,  $J$  is the exchange constant,  $\delta$  is the anisotropy parameter,  $g$  is the strength of the transverse magnetic field,  $\hbar$  is the Planck constant reduce,  $\otimes$  is the tensor product between two operator and  $L$  is the length of the lattice. The Dzyaloshinskii-Moriya interaction (DMI) adds another term to the Hamiltonian, represented by:

$$\hat{\mathcal{H}}_D = D\hbar \sum_{n=1}^L \left( \sigma_n^x \otimes \sigma_{n+1}^y + \gamma \sigma_n^y \otimes \sigma_{n+1}^x \right), \quad (3)$$

where  $D$  is the DMI constant and  $\gamma$  is a correction factor associated with the DMI. Therefore, the Hamiltonian for the 1D lattice that we study is:

$$\hat{\mathcal{H}} = \hat{\mathcal{H}}_{XY} + \hat{\mathcal{H}}_D. \quad (4)$$

To get a schematic the system we will study in [Figure 1](#)

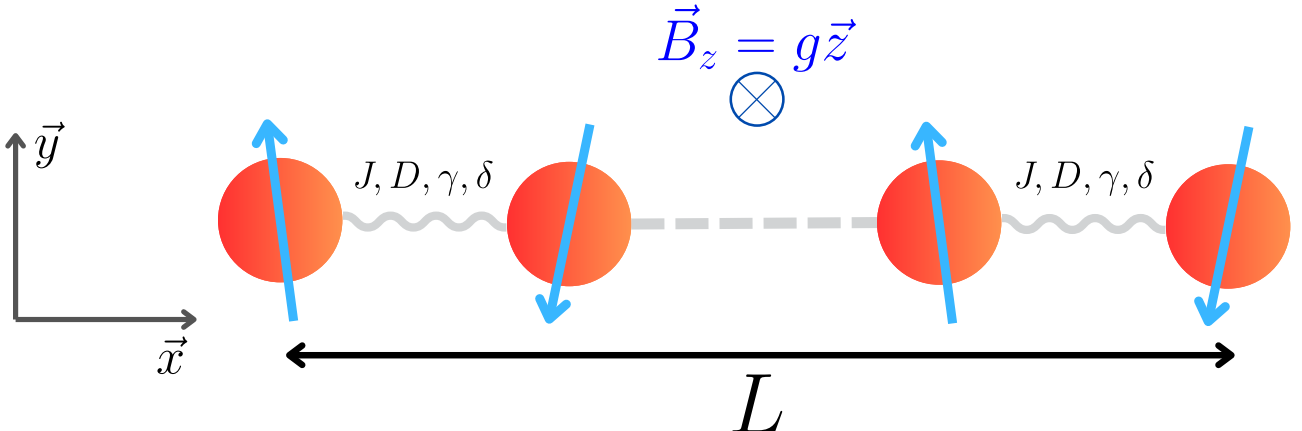


Figure 1: Schematic of the lattice of  $L+1$  qubits with the Heisenberg XY model and DMI, where the blue arrows represent the spin states of the qubits, and the gray waves represent the interaction between two neighboring qubits.

## 2. Methodology

The goal here is to compute the time evolution of the concurrence  $C(\rho(t))$  in the lattice as shown in [Figure 1](#), with the Hamiltonian of the XY model and DMI. To achieve this, we have two approaches: a numerical approach using the Python programming language and an analytical approach.

### 2.1 Numerical approach

To simulate the evolution of the concurrence [Definition 1](#), we need to compute the density matrix. However, the necessary condition to compute the density matrix  $\rho(t)$  is to find the state of the quantum system at time  $t$ . For this purpose, we use the postulate of the evolution of the quantum system given by the Schrödinger equation [\[3\]](#).

$$\forall t \in \mathbb{R}_+, i\hbar\partial_t |\psi(t)\rangle = \hat{\mathcal{H}}(t) |\psi(t)\rangle \quad (5)$$

Now let's explain a generic algorithm to solve the Schrödinger equation.

First, let's introduce the evolution operator  $\mathcal{U}(t, t_0)$  which maps the initial state  $|\psi(t_0)\rangle$  of the system to the state  $|\psi(t)\rangle$  at time  $t$ :

$$\forall t \in \mathbb{R}_+, |\psi(t)\rangle = \mathcal{U}(t, t_0) |\psi(t_0)\rangle \text{ with } \mathcal{U}(t, t_0)\mathcal{U}(t, t_0)^\dagger = \mathcal{U}(t, t_0)^\dagger\mathcal{U}(t, t_0) = \text{id} \quad (6)$$

where id is the identity operator and  $\mathcal{U}^\dagger(t, t_0)$  is the adjoint of  $\mathcal{U}(t, t_0)$ . Now, let's consider a Hamiltonian  $\hat{\mathcal{H}}(t)$  which is piecewise constant, i.e.,

$$\forall j \in \mathbb{N}, \hat{\mathcal{H}}(t) = \hat{\mathcal{H}}(t_j) \quad \text{for} \quad t_j < t < t_{j+1}, \quad (7)$$

where  $t_j$  are time steps at which the Hamiltonian changes suddenly.

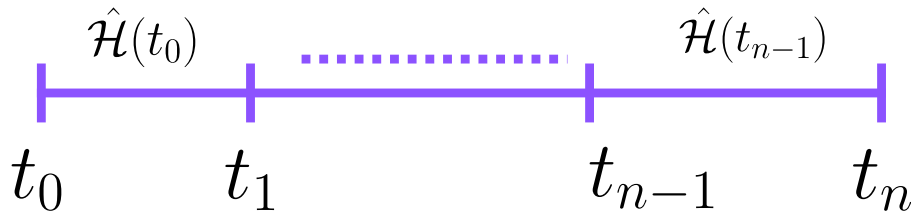


Figure 2: Schematic of the [Proposition 7](#)

With the hypothesis in [Proposition 7](#), the evolution operator in [Definition 6](#), and the Schrödinger equation in [Equation 5](#), we can express the evolution operator  $\mathcal{U}(t, t_0)$  as:

$$\mathcal{U}(t, t_0) = e^{-i\hat{\mathcal{H}}(t-t_0)/\hbar} \quad (8)$$

With the hypothesis in [Proposition 7](#), the evolution operator in [Definition 6](#), and the Schrödinger equation in [Equation 5](#), we can express the evolution operator  $\mathcal{U}(t, t_0)$  as:

$$\begin{aligned}
 |\psi(t_1)\rangle &= e^{-i\hat{\mathcal{H}}(t_0)(t_1-t_0)/\hbar} |\psi(t_0)\rangle \\
 |\psi(t_2)\rangle &= e^{-i\hat{\mathcal{H}}(t_1)(t_2-t_1)/\hbar} |\psi(t_1)\rangle = e^{-i\hat{\mathcal{H}}(t_1)(t_2-t_1)/\hbar} e^{-i\hat{\mathcal{H}}(t_0)(t_1-t_0)/\hbar} |\psi(t_0)\rangle \\
 &\vdots \\
 |\psi(t_n)\rangle &= e^{-i\hat{\mathcal{H}}(t_{n-1})(t_n-t_{n-1})/\hbar} |\psi(t_{n-1})\rangle \cdots e^{-i\hat{\mathcal{H}}(t_0)(t_2-t_1)/\hbar} e^{-i\hat{\mathcal{H}}(t_1-t_0)/\hbar} |\psi(t_0)\rangle
 \end{aligned}$$

Let us consider equally spaced time intervals:

$$t_j = t_0 + j\Delta t.$$

Thus, the state of the quantum system at time  $t_n$  is:

$$\forall n \in \mathbb{N}^*, |\psi(t_n)\rangle = \prod_{i=0}^{n-1} e^{-i\hat{\mathcal{H}}(t_i)\Delta t/\hbar} |\psi(t_0)\rangle \quad (9)$$

Notice the temporal order of operators  $\mathcal{U}(t_j, t_{j-1})$  with  $t_j > t_{j-1}$ . Operators later in time appear to the left.

From this, we can deduce the following algorithm to solve the Schrödinger equation:

---

### Algorithm 1 Solve Time-Dependent Schrödinger Equation

---

```

1: procedure SOLVE( $n$  : integer,  $t_f$  : integer, Hamil: function,  $|\psi(t_0)\rangle$  : array)
2:    $\Delta t \leftarrow \frac{t_f}{n}$ 
3:   times  $\leftarrow$  linspace( $0, t_f, n$ )
4:   state_t  $\leftarrow$  empty list
5:   for  $j = 0$  to length of times  $- 1$  do
6:      $\hat{\mathcal{H}}(t_j) \leftarrow$  Hamil(times[ $j$ ])
7:      $\mathcal{U}(t_{j+1} - t_j) \leftarrow$  matrix_exponential( $(-i \times \hat{\mathcal{H}}(t_j) \times \Delta t)$ )
8:      $|\psi(t_{j+1})\rangle \leftarrow$  matrix_dot_product( $\mathcal{U}(t_{j+1} - t_j), |\psi(t_0)\rangle$ )
9:     append  $|\psi(t_{j+1})\rangle$  to state_t
10:     $|\psi(t_0)\rangle \leftarrow |\psi(t_{j+1})\rangle$ 
11:   end for
12:   return state_t
13: end procedure

```

---

Now we can compute the density matrix at time  $t$ . However, if the length of the lattice is  $L > 1$ , we cannot compute  $C(\rho(t))$  directly according to the definition of concurrence **Definition 1**, which applies to only two qubits. If  $L > 1$ , there are more than two qubits in the lattice, so the standard definition of concurrence cannot be used. Let's examine an example with three qubits to understand this problem, as shown in the following figure:

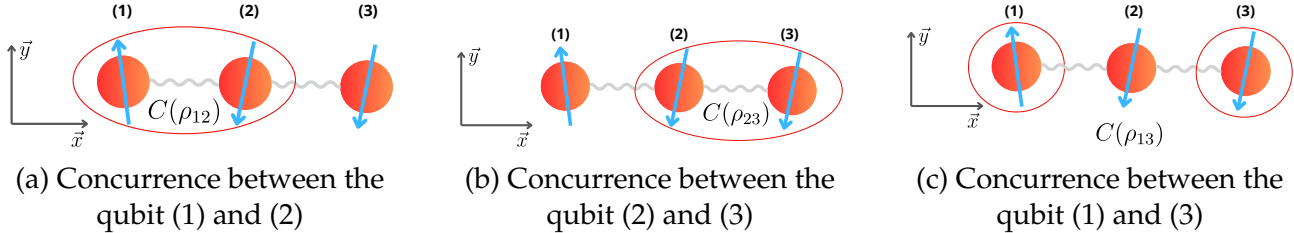


Figure 3: Problem of calculation of the concurrence for many qubits

As seen in 3, we need to isolate pairs of qubits and compute the density matrix of each pair, denoted as  $\rho_{ij}$  where  $i \neq j$  and  $(i, j) \in \mathbb{N}^*$ . For this, we use a mathematical tool called the partial trace [2].

Let  $A$  and  $B$  be two subsystems making up the composite system described by the density operator  $\rho_{AB} \in \mathcal{M}_{2^N}(\mathbb{C})$ . Let note  $\dim(\mathcal{H}_A) = d_A$  and  $\dim(\mathcal{H}_B) = d_B$ .

The partial trace over the  $B$  subsystem, denoted  $\text{Tr}_B$ , is defined as

$$\text{Tr}_B[\rho_{AB}] := \sum_j^{d_B} (\hat{\mathbb{I}}_{d_A}^{(A)} \otimes \langle j|_B) \rho_{AB} (\hat{\mathbb{I}}_{d_A}^{(A)} \otimes |j\rangle_B), \quad (10)$$

where  $\{|j\rangle\}$  is any orthonormal basis for the Hilbert space  $\mathcal{H}_B$  of subsystem  $B$ . We often write  $\rho_A \equiv \text{Tr}_B[\rho_{AB}] \in \mathcal{M}_{2^{(N-1)}}(\mathbb{C})$  and  $\hat{\mathbb{I}}_{d_A}^{(A)}$  the identity matrix size  $d_A$ .

Similarly, the partial trace over the  $A$  subsystem, denoted  $\text{Tr}_A$ , is defined as

$$\text{Tr}_A[\rho_{AB}] := \sum_j^{d_A} (\langle i|_A \otimes \hat{\mathbb{I}}_{d_B}^{(B)}) \rho_{AB} (|i\rangle_A \otimes \hat{\mathbb{I}}_{d_B}^{(B)}), \quad (11)$$

where  $\{|i\rangle\}$  is any orthonormal basis for the Hilbert space  $\mathcal{H}_A$  of subsystem  $A$ . We often write  $\rho_B \equiv \text{Tr}_A[\rho_{AB}] \in \mathcal{M}_{2^{(N-1)}}(\mathbb{C})$  and  $\hat{\mathbb{I}}_{d_B}^{(B)}$  the identity matrix size  $d_B$ .

### 3. Results And Discussion

#### 3.1 Entanglement in a spin chain with 2 qubits

In this section, we analyze the dynamics of a system consisting of two qubits with the Hamiltonian given by:

$$\hat{\mathcal{H}} = \hbar J \left[ \left( \frac{1+\delta}{2} \right) \sigma_1^x \otimes \sigma_2^x + \left( \frac{1-\delta}{2} \right) \sigma_1^y \otimes \sigma_2^y \right] + D\hbar (\sigma_1^x \otimes \sigma_2^y + \gamma \sigma_1^y \otimes \sigma_2^x) + g (\sigma_1^z \otimes \hat{\mathbb{I}} + \hat{\mathbb{I}} \otimes \sigma_2^z).$$

we focus on the concurrence  $C(\rho(t))$ , which quantifies the entanglement between the two qubits. The analytical solution for the concurrence, as derived in Appendix B, is given by:

$$C(\rho(t)) = |\sin(2\mu t)|,$$

where  $\mu = \sqrt{J^2 + D^2(\gamma - 1)^2}$ .

We plot the concurrence in the figure

We can see the plot of  $C(|\psi(t)\rangle)$  for the  $|\psi(t)\rangle$  at [Equation 24](#) in the figure

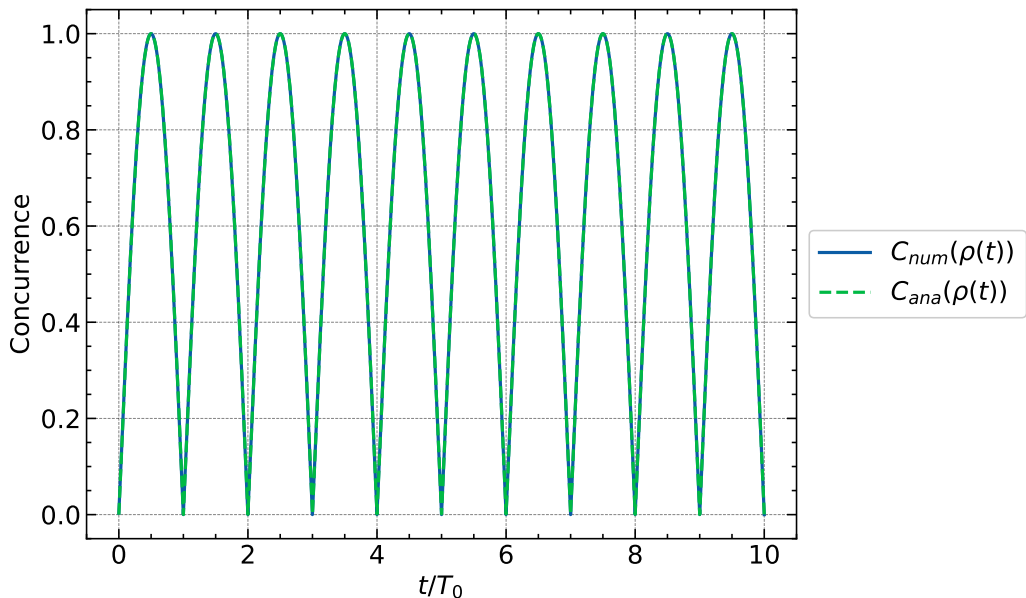


Figure 4:  $D = 0$ , Mean Squared Error: 1.51e-07,  $\gamma = -1$ ,  $\delta = 1$ ,  $g = 1$ ,  $J = 1$

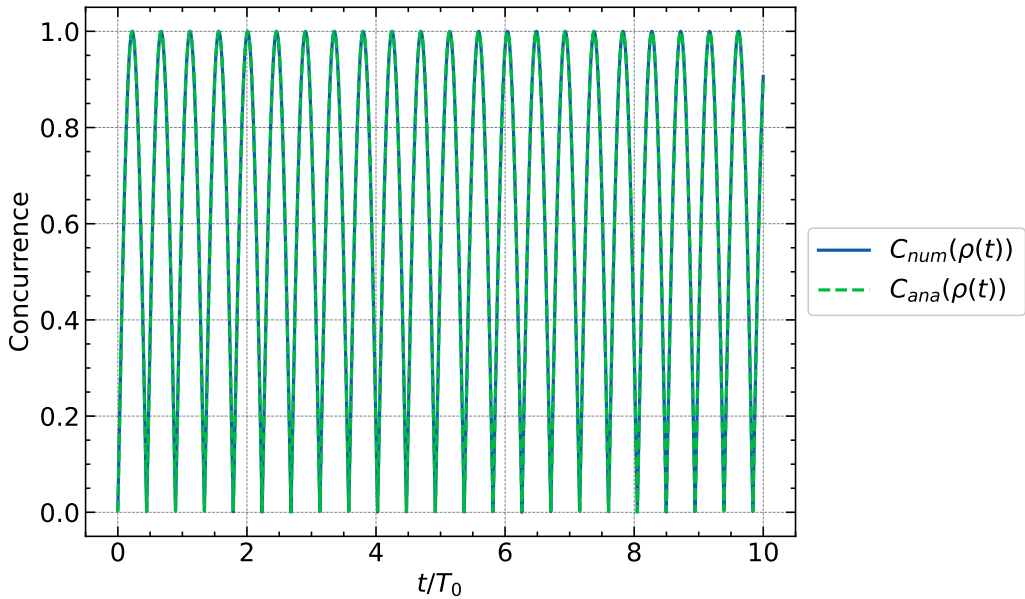


Figure 5:  $D = 1$ , Mean Squared Error:  $1.51\text{e-}07$ ,  $\gamma = -1$ ,  $\delta = 1$ ,  $g = 1$ ,  $J = 1$

The concurrence formula reveals a simple yet profound oscillatory behavior of the entanglement between the qubits. The parameter  $\mu$  plays a crucial role in determining the frequency of these oscillations, which depends on the coupling constants  $J$  and  $D$  as well as the anisotropy parameter  $\gamma$ .

#### **Impact of Coupling Constants $J$ and $D$ :**

The coupling constant  $J$  directly contributes to  $\mu$ , indicating that a stronger XX and YY interaction leads to faster oscillations in concurrence. The term  $D(\gamma - 1)$  suggests that the effect of the  $D$  coupling on the concurrence is modulated by the anisotropy  $\gamma$ . For  $\gamma = 1$ , this contribution vanishes, and the oscillation frequency is solely determined by  $J$ . However, for  $\gamma \neq 1$ , the anisotropy introduces additional dynamics through  $D$ .

#### **Behavior for Different Regimes of $\mu$ :**

When  $\mu$  is large (e.g., large  $J$  or significant anisotropy), the concurrence oscillates rapidly, meaning that the system frequently transitions between entangled and separable states. For small  $\mu$ , the oscillations are slower, indicating more prolonged periods of either high or low entanglement.

**Maximal Concurrence:** The concurrence achieves its maximum value of 1 when  $\sin(2\mu t) = \pm 1$ , indicating a fully entangled state. Conversely,  $C(\rho(t)) = 0$  when  $\sin(2\mu t) = 0$ , representing separable states where the qubits are not entangled.

## 3.2 Discussion

The results provide significant insights into the entanglement dynamics in a two-qubit system with anisotropic and cross-coupling terms. The oscillatory nature of the concurrence reflects the intricate interplay between different types of interactions present in the Hamil-

tonian. This behavior is essential for applications in quantum information processing, where control over entanglement is crucial.

- **Quantum Control:** By tuning the parameters  $J$ ,  $D$ , and  $\gamma$ , one can manipulate the entanglement dynamics, potentially allowing for the design of specific quantum gates or the implementation of quantum error correction protocols that rely on dynamic entanglement.
- **Effect of Anisotropy:** The dependence of  $\mu$  on  $\gamma$  illustrates how anisotropy can either enhance or diminish the contribution of the  $D$  coupling to the entanglement dynamics. This result suggests that systems with tunable anisotropy could be particularly versatile in quantum control schemes.
- **Robustness of Entanglement:** The periodic nature of the concurrence indicates that, under specific conditions, entanglement can be robust over time, recurring predictably as a function of time. This property might be exploited to maintain entanglement over long durations in quantum communication protocols.

In Conclusion concurrence quantifies the entanglement between two qubits. For example, when  $t/T_0 = 0.5 + k$ , where  $k \in \mathbb{N}$ , the concurrence is 1. At this time, the state  $|\psi(t)\rangle$  is:

$$|\psi\left(t = \frac{\pi}{4} + \frac{k\pi}{2}\right)\rangle = \frac{1}{\sqrt{2}} |\uparrow\downarrow\rangle - \frac{i(J + iD(\gamma - 1))}{\sqrt{2}\gamma} |\downarrow\uparrow\rangle$$

This state is evidently entangled according to the definition.

Moreover we can recognize a Bell state we this form:

$$|\psi\left(t = \frac{\pi}{4} + \frac{k\pi}{2}\right)\rangle = \frac{1}{\sqrt{2}} (|\uparrow\downarrow\rangle - ie^{i\theta} |\downarrow\uparrow\rangle) \quad (12)$$

where  $\theta = \arctan\left(\frac{D(\gamma-1)}{J}\right)$

And at  $t/T_0 = k$  the concurrence equal to 0,

$$|\psi\left(t = \frac{k\pi}{2}\right)\rangle = \frac{i(J + iD(\gamma - 1))}{\sqrt{2}\gamma} |\downarrow\uparrow\rangle$$

In this case, the state is separable.

### 3.3 Entanglement in a spin chain with N qubits

This study systematically investigates the concurrence in a three-qubit system and a six-qubit system governed by the Heisenberg XY model, incorporating the Dzyaloshinskii-Moriya interaction (DMI). The primary parameters analyzed include the DMI constant  $D$ , the anisotropy parameter  $\delta$ , and the correction factor  $\gamma$ . The concurrence between pairs of qubits was assessed under various configurations of these parameters.

#### 3.3.1 Entanglement in a spin chain with 3 qubits

The concurrence values varied from 0.0 to approximately 0.8, indicating robust entanglement within the qubit system. The pairwise concurrences ( $C_{1,2}, C_{1,3}, C_{2,3}$ ) exhibited a consistent pattern, with entanglement gradually diminishing over time.

In the first subfigure [Figure 6a](#), the concurrence values show a peak of approximately 0.8 with  $D = 0$ ,  $\gamma = 1$ , and  $\delta = 0$ . With an increase in the anisotropy parameter to  $\delta = 1$  [Figure 6b](#), the concurrence values remained relatively high, albeit slightly lower than in the previous case. The maximum concurrence observed was around 0.6, with a similar temporal decline in entanglement distribution across the qubits.

The introduction of DMI with  $D = 1$  [Figure 6c](#) resulted in a slight enhancement of concurrence values, reaching a peak of approximately 0.8. This suggests that DMI strengthens the entanglement between qubits, with the pairwise concurrences following a similar pattern to earlier configurations but with marginally higher values.

When both  $D$  and  $\delta$  were set to 1 [Figure 6d](#), the concurrence values were slightly lower, peaking at about 0.6. The entanglement distribution remained similar across qubit pairs, though the overall entanglement was reduced compared to the scenario with  $D = 1$  and  $\delta = 0$ .

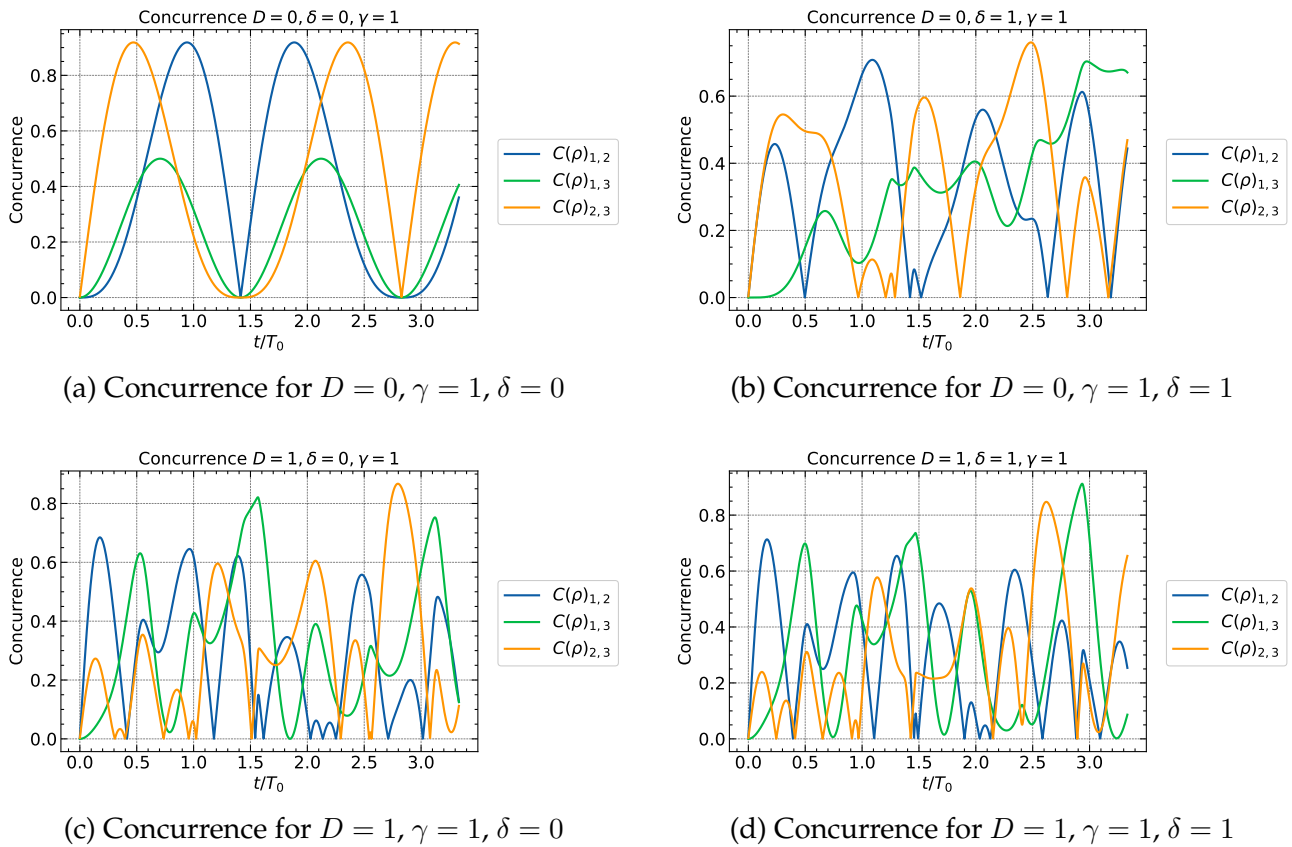


Figure 6: Concurrence for different values of  $D$  and  $\delta$  with  $\gamma = 1$ . The concurrence values indicate the level of entanglement in the qubit system over time, showing how different parameters influence the entanglement.

### Discussion

The findings highlight the significant role of the Dzyaloshinskii-Moriya interaction in influencing the entanglement characteristics of the three-qubit system. The DMI, quantified by  $D$ , generally enhances concurrence, indicating stronger entanglement. This effect is particularly pronounced when comparing scenarios with  $D = 0$  and  $D = 1$ .

Conversely, the anisotropy parameter  $\delta$  introduces a competing influence that can diminish the overall entanglement as it increases. Specifically, when  $\delta = 1$ , the system exhibits lower concurrence values compared to  $\delta = 0$ , even in the presence of DMI. This suggests that while DMI tends to enhance entanglement, increasing  $\delta$  may counteract this effect, possibly due to modifications in the system's symmetry or interaction strengths.

In the absence of DMI ( $D = 0$ ), the system still demonstrates significant entanglement, especially when  $\gamma = 1$  and  $\delta = 0$ , with concurrence values reaching up to 0.8. This indicates that the Heisenberg XY model inherently supports strong entanglement, which can be modulated by adjusting the DMI and anisotropy parameters.

### 3.3.2 Entanglement in a spin chain with 6 qubits

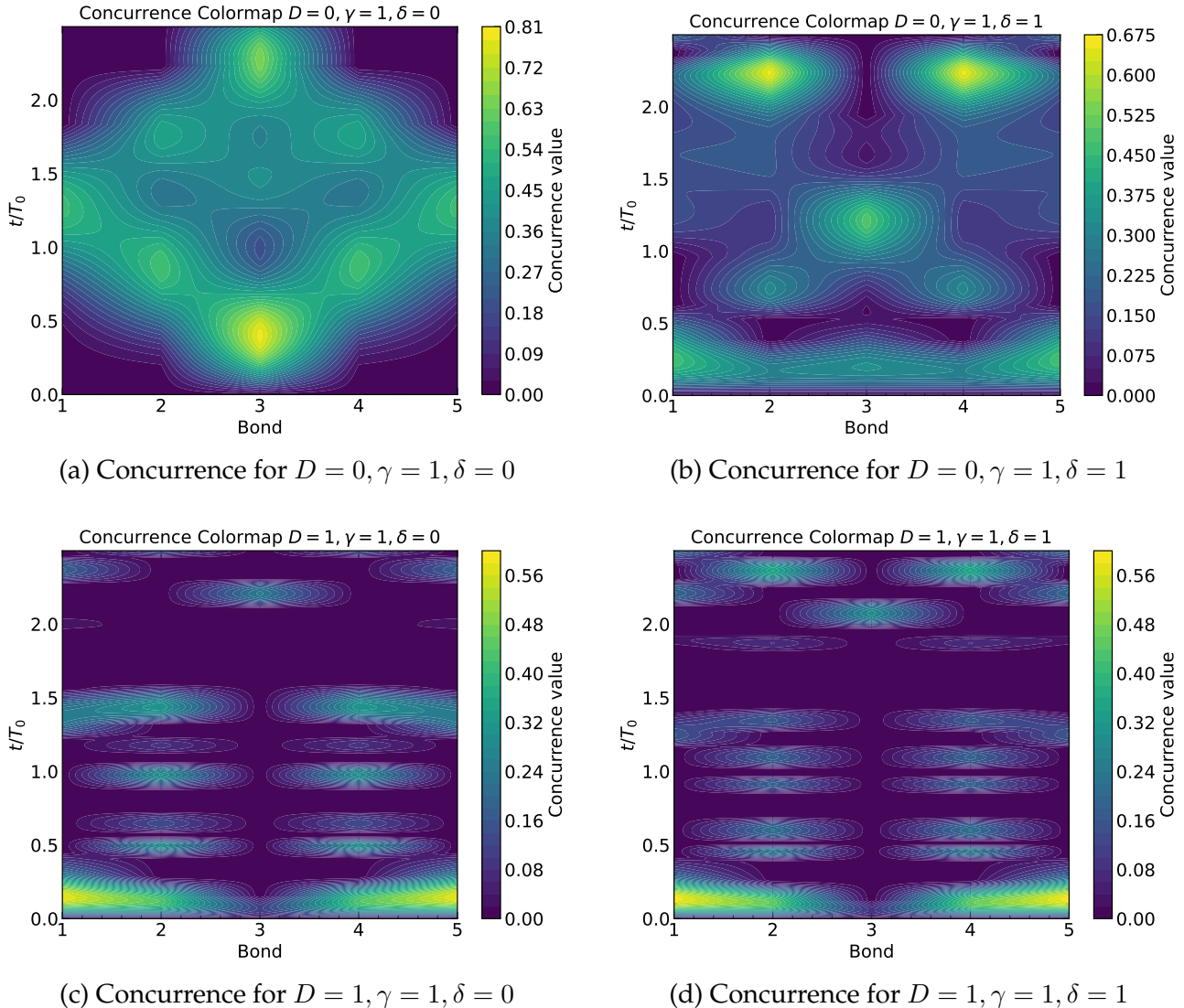


Figure 7: Concurrence for different values of  $D$  and  $\delta$  with  $\gamma = 1$  in a 6-qubit system. The plots illustrate how these parameters affect the entanglement within the system over time.

**Concurrence for  $D = 0, \gamma = 1, \delta = 0$ :** [Figure 7a](#) The concurrence values in this configuration range from 0.00 to approximately 0.81, showing a high level of entanglement that gradually decreases as the system evolves over time. The colormap indicates a relatively uniform distribution of entanglement across the bonds in the lattice.

**Concurrence for  $D = 0, \gamma = 1, \delta = 1$ :** [Figure 7b](#) When  $\delta$  is increased to 1, the maximum concurrence value decreases slightly to approximately 0.675. The distribution of concurrence values remains similar to the previous case, with the entanglement decreasing over time, but with a slightly reduced maximum entanglement value.

**Concurrence for  $D = 1, \gamma = 1, \delta = 0$ :** [Figure 7a](#) Introducing the DMI constant  $D = 1$  while keeping  $\gamma = 1$  and  $\delta = 0$  leads to an increase in the maximum concurrence value

to around 0.81. This increase suggests that the DMI enhances the entanglement within the system. The distribution of concurrence is still fairly uniform across the lattice, indicating that the DMI positively influences the overall entanglement.

**Concurrence for  $D = 1, \gamma = 1, \delta = 1$ :** [Figure 7d](#) When both  $D$  and  $\delta$  are set to 1, the system exhibits a maximum concurrence value of approximately 0.56, which is lower than when  $\delta = 0$ . This suggests that while the DMI increases entanglement, the anisotropy parameter  $\delta$  introduces an effect that reduces the overall entanglement when  $\gamma$  is also present.

The results indicate that the Dzyaloshinskii-Moriya interaction (DMI) significantly influences the entanglement properties of the system. Specifically, the concurrence values increase when the DMI constant  $D$  is set to 1, implying that the DMI fosters stronger entanglement between the qubits in the lattice. This enhancement is evident when comparing cases with  $D = 0$  and  $D = 1$ , where the latter consistently shows higher concurrence values.

However, the anisotropy parameter  $\delta$  and the correction factor  $\gamma$  introduce competing effects. When  $\delta = 1$  and  $\gamma = 1$ , the concurrence is lower compared to when  $\delta = 0$  and  $\gamma = 1$ , even in the presence of DMI. This reduction suggests that the anisotropy, along with  $\gamma$ , can counteract the positive impact of DMI on entanglement. The interplay between these parameters likely alters the symmetry and interaction strength within the lattice, thereby influencing the entanglement.

In scenarios where  $D = 0$ , the system still exhibits significant entanglement, particularly when  $\gamma = 1$  and  $\delta = 0$ , with concurrence values reaching up to approximately 0.81. This demonstrates that the Heisenberg XY model itself supports strong entanglement, but this can be modulated by the presence of DMI and adjustments to  $\delta$  and  $\gamma$ .

# Conclusion

This study provides a comprehensive analysis of the entanglement properties in both 2-qubit, 3-qubit and 6-qubit systems modeled by the Heisenberg XY Hamiltonian with Dzyaloshinskii-Moriya interaction (DMI). The key findings from our analysis can be summarized as follows:

1. **Impact of Dzyaloshinskii-Moriya Interaction (DMI):** The presence of the DMI, represented by the parameter  $D$ , consistently enhances the entanglement between qubits. This is observed through increased concurrence values in both the 2-qubit, 3-qubit and 6-qubit systems when  $D = 1$  compared to when  $D = 0$ . The DMI facilitates stronger quantum correlations, making it a valuable tool for increasing entanglement in quantum systems.
2. **Effect of Anisotropy Parameter  $\delta$ :** The anisotropy parameter  $\delta$  introduces a counter-acting influence on the entanglement. While the system shows high concurrence values when  $\delta = 0$ , an increase in  $\delta$  generally leads to a reduction in these values, especially in the presence of DMI. This suggests that  $\delta$  affects the symmetry and interaction strengths within the lattice, reducing the overall entanglement when increased.

In conclusion, the Dzyaloshinskii-Moriya interaction and the anisotropy parameter provide powerful mechanisms for manipulating entanglement in quantum systems. Understanding how these parameters influence entanglement allows for the precise control of the quantum system, which has significant implications for the development of quantum technologies. This study lays the groundwork for future research into optimizing entanglement in more complex quantum systems and exploring the practical applications of these findings in quantum computing and materials science.

# References

- [1] Charles H. Bennett, Gilles Brassard, Claude Crépeau, Richard Jozsa, Asher Peres, and William K. Wootters. Teleporting an unknown quantum state via dual classical and Einstein-Podolsky-Rosen channels. *Physical Review Letters*, 70(13):1895–1899, March 1993. Publisher: American Physical Society.
- [2] Tai-Danae Bradley. At the Interface of Algebra and Statistics, April 2020. arXiv:2004.05631 [quant-ph, stat].
- [3] C. Cohen-Tannoudji, B. Diu, and F. Laloë. *Quantum Mechanics, Volume 2: Angular Momentum, Spin, and Approximation Methods*. Wiley, 2019.
- [4] I. Dzyaloshinsky. A thermodynamic theory of “weak” ferromagnetism of antiferromagnetics. *Journal of Physics and Chemistry of Solids*, 4(4):241–255, January 1958.
- [5] Ryszard Horodecki, Paweł Horodecki, Michał Horodecki, and Karol Horodecki. Quantum entanglement. *Reviews of Modern Physics*, 81(2):865–942, June 2009. arXiv:quant-ph/0702225.
- [6] Tōru Moriya. Anisotropic Superexchange Interaction and Weak Ferromagnetism. *Physical Review*, 120(1):91–98, October 1960. Publisher: American Physical Society.
- [7] S. Pirandola, U. L. Andersen, L. Banchi, M. Berta, D. Bunandar, R. Colbeck, D. Englund, T. Gehring, C. Lupo, C. Ottaviani, J. Pereira, M. Razavi, J. S. Shaari, M. Tomamichel, V. C. Usenko, G. Vallone, P. Villoresi, and P. Wallden. Advances in Quantum Cryptography. *Advances in Optics and Photonics*, 12(4):1012, December 2020. arXiv:1906.01645 [math-ph, physics:physics, physics:quant-ph].
- [8] A. J. van der Sijs. Heisenberg models and a particular isotropic model. *Physical Review B*, 48(10):7125–7133, September 1993. Publisher: American Physical Society.
- [9] James D. Whitfield, Jun Yang, Weishi Wang, Joshua T. Heath, and Brent Harrison. Quantum Computing 2022, June 2022. arXiv:2201.09877 [quant-ph].
- [10] William K. Wootters. Entanglement of Formation of an Arbitrary State of Two Qubits. *Physical Review Letters*, 80(10):2245–2248, March 1998. arXiv:quant-ph/9709029.

# Appendices

<b>A Appendix A</b>	<b>i</b>
A.1 Generalities and Recall on Matrix Series . . . . .	i
A.2 Properties exponential of matrix . . . . .	ii
<b>B Appendix B</b>	<b>v</b>
<b>C Appendix C</b>	<b>ix</b>

## A. Appendix A

### A.1 Generalities and Recall on Matrix Series

#### Definition 1: Norme matrix

For  $A = (a_{ij}) \in M_n(\mathbb{C})$ , we define

$$\|A\|_\infty = \max\{|a_{ij}|; 1 \leq i, j \leq n\}.$$

$\|\cdot\|_\infty$  is a norm on  $M_n(\mathbb{C})$ , i.e., it is a function with values in  $\mathbb{R}^+$  such that

- $\forall A, \|A\|_\infty = 0 \iff A = 0$ ,
- $\forall A, \forall \lambda \in \mathbb{C}, \|\lambda A\|_\infty = |\lambda| \cdot \|A\|_\infty$ ,
- $\forall A, B, \|A + B\|_\infty \leq \|A\|_\infty + \|B\|_\infty$ .

In the following, we will denote  $\|\cdot\|$  instead of  $\|\cdot\|_\infty$ .

#### Definition 2: Converge sequence of matrix

- A sequence  $(A_k)$  of  $M_n(\mathbb{C})$  is said to be convergent if there exists  $A \in M_n(\mathbb{C})$  such that  $\forall \epsilon > 0, \exists k_0 \in \mathbb{N}$  such that  $k \geq k_0 \Rightarrow \|A_k - A\| < \epsilon$ .
- A sequence  $(A_k)$  is said to be Cauchy if  $\forall \epsilon > 0, \exists k_0 \in \mathbb{N}, \forall k, k_0 \geq k_0, \|A_k - A_{k_0}\| < \epsilon$ .

#### Proposition 1: Characterization of matrix convergence

Let  $(A_k)$  be a sequence of  $M_n(\mathbb{C})$ . Then it is Cauchy if and only if it is convergent.

*Proof.* The right-to-left direction is classical, and the direct direction relies on the completeness of  $\mathbb{C}$  □

**Definition 3: Convergent and Absolutely convergent matrix serie**

Given a sequence  $(A_k)$  of  $M_n(\mathbb{C})$ , we define the associated series denoted  $\sum A_k$  as the sequence  $(S_k)$  with general term

$$S_k = \sum_{l=0}^k A_l.$$

The series is said to be absolutely convergent if the real series  $\sum \|A_k\|$  is convergent.

**Proposition 2: Convergent and Absolutely convergent matrix serie**

If  $\sum A_k$  is absolutely convergent, then it is convergent.

*Proof.* Let  $\epsilon > 0$ . For all  $k \in \mathbb{N}$ , denote  $T_k = \sum_{l=0}^k \|A_l\|$  and  $S_k = \sum_{l=0}^k A_l$ . By hypothesis,  $(T_k)$  converges (in  $\mathbb{R}$ ), so it is Cauchy. Hence, there exists  $k_0 \in \mathbb{N}$  such that for  $k, k_0 \geq k_0$ , we have  $|T_k - T_{k_0}| < \epsilon$ .

For  $k_0 \geq k \geq k_0$ , we have

$$\|S_{k_0} - S_k\| = \left\| \sum_{l=k+1}^{k_0} A_l \right\| \leq \sum_{l=k+1}^{k_0} \|A_l\| = T_{k_0} - T_k < \epsilon.$$

Thus, the sequence  $(S_k)$  is Cauchy, hence convergent.  $\square$

**Lemma 1: Matrix inequality**

For  $A, B \in M_n(\mathbb{C})$ ,

$$\|AB\| \leq n\|A\|\|B\| \quad \text{and} \quad \|A^k\| \leq n^{k-1}\|A\|^k.$$

*Proof.* Let  $A = (a_{ij})$ ,  $B = (b_{ij})$ , and  $C = AB = (c_{ij})$ . For all  $i, j$ ,

$$|c_{ij}| = \left| \sum_{k=1}^n a_{ik} b_{kj} \right| \leq \sum_{k=1}^n |a_{ik}| |b_{kj}| \leq \sum_{k=1}^n \|A\| \|B\| = n\|A\|\|B\|.$$

Consequently,  $\|C\| \leq n\|A\|\|B\|$ .

The second inequality is obtained by induction on  $k$  using the first.  $\square$

## A.2 Properties exponential of matrix

**Definition 4: Exponential of matrix**

Let  $A \in M_n(\mathbb{C})$ . We define  $e^A = \exp(A) \in M_n(\mathbb{C})$  by

$$e^A = \sum_{k=0}^{+\infty} \frac{A^k}{k!}.$$

**Theorem 1: Existence of the exponential of matrix**

The series  $\sum \frac{A^k}{k!}$  converges. Thus, the matrix  $e^A$  is well-defined.

*Proof.* If  $A = 0$ , it is trivial. We assume  $A$  is non-zero. We show that the series is absolutely convergent. Indeed,

$$\left\| \sum_{l=0}^k \frac{A^l}{l!} \right\| \leq \sum_{l=0}^k \frac{n^{l-1} \|A\|^l}{l!}.$$

Let  $u_l = \frac{n^{l-1} \|A\|^l}{l!}$ . Then  $\frac{u_{l+1}}{u_l} = \frac{n \|A\|}{l+1}$  and this tends to 0 as  $l$  tends to  $+\infty$ . By the D'Alembert criterion, the series  $\sum u_l$  is convergent, which implies the absolute convergence of our original series.  $\square$

**Theorem 2: Matrix exponential and Pauli matrices**

Let the matrix  $\vec{\sigma} = \hat{\sigma}^x \hat{x} + \hat{\sigma}^y \hat{y} + \hat{\sigma}_z \hat{z}$  and the vector  $\hat{n} = a\hat{x} + b\hat{y} + c\hat{z}$ , where  $(\hat{x}, \hat{y}, \hat{z})$  is an orthonormal basis. The  $\sigma_a$  are the Pauli matrices for  $a \in \{x, y, z\}$ .

If  $\|\hat{n}\| = 1$  then :

$$e^{i\mu(\hat{n} \cdot \vec{\sigma})} = \hat{\mathbb{I}} \cos(\mu) + i(\hat{n} \cdot \vec{\sigma}) \sin(\mu). \quad (13)$$

where  $\cdot$  : is the inner product in  $\mathbb{R}^3$

*Proof.* Exponential of a Pauli vector:

For

$$\vec{\mu} = \mu \hat{n}, \quad |\hat{n}| = 1,$$

one has, for even powers,  $2p, p = 0, 1, 2, 3, \dots$

$$(\hat{n} \cdot \vec{\sigma})^{2p} = I,$$

which can be shown first for the  $p = 1$  case using the anticommutation relations. For convenience, the case  $p = 0$  is taken to be  $I$  by convention.

For odd powers,  $2q + 1, q = 0, 1, 2, 3, \dots$

$$(\hat{n} \cdot \vec{\sigma})^{2q+1} = \hat{n} \cdot \vec{\sigma}.$$

Matrix exponentiating, and using the Taylor series for sine and cosine,

$$\begin{aligned}
 e^{i\mu(\hat{n}\cdot\vec{\sigma})} &= \sum_{k=0}^{\infty} \frac{i^k [\mu(\hat{n}\cdot\vec{\sigma})]^k}{k!} \\
 &= \sum_{p=0}^{\infty} \frac{(-1)^p (\mu\hat{n}\cdot\vec{\sigma})^{2p}}{(2p)!} + i \sum_{q=0}^{\infty} \frac{(-1)^q (\mu\hat{n}\cdot\vec{\sigma})^{2q+1}}{(2q+1)!} \\
 &= I \sum_{p=0}^{\infty} \frac{(-1)^p \mu^{2p}}{(2p)!} + i(\hat{n}\cdot\vec{\sigma}) \sum_{q=0}^{\infty} \frac{(-1)^q \mu^{2q+1}}{(2q+1)!}.
 \end{aligned}$$

In the last line, the first sum is the cosine, while the second sum is the sine; so, finally,

$$e^{i\mu(\hat{n}\cdot\vec{\sigma})} = \hat{\mathbb{I}} \cos \mu + i(\hat{n}\cdot\vec{\sigma}) \sin \mu.$$

□

## B. Appendix B

The objective of this section is to solve the Schrödinger equation for a chain of two qubits:

$$\begin{cases} i\hbar\partial_t |\psi(t)\rangle = \hat{\mathcal{H}} |\psi(t)\rangle \\ |\psi(t=0)\rangle = |\uparrow\downarrow\rangle \end{cases}$$

The Hamiltonian of this system is given by:

$$\hat{\mathcal{H}} = \hat{\mathcal{H}}_{XY} + \hat{\mathcal{H}}_D \quad (14)$$

$$\hat{\mathcal{H}}_{XY} = \hbar J \left[ \left( \frac{1+\delta}{2} \right) \sigma_x^{(1)} \otimes \sigma_x^{(2)} + \left( \frac{1-\delta}{2} \right) \sigma_y^{(1)} \otimes \sigma_y^{(2)} \right] + \hbar g \sigma_z^{(1)} \otimes \hat{\mathbb{I}}_2^{(2)} \quad (15)$$

and

$$\hat{\mathcal{H}}_D = D\hbar \left( \sigma_x^{(1)} \otimes \sigma_y^{(2)} + \gamma \sigma_y^{(1)} \otimes \sigma_x^{(2)} \right) \quad (16)$$

Now let define the Hilbert space of the quantum system of two qubits, first of all the Hilbert basis of the first qubit ( $\mathcal{H}_1$ : Hilbert space of the first qubit) is given by:

$$|\uparrow\rangle^{(1)} = \begin{pmatrix} 1 \\ 0 \end{pmatrix} \text{ and } |\downarrow\rangle^{(1)} = \begin{pmatrix} 0 \\ 1 \end{pmatrix}$$

then the Hilbert basis of the second qubit ( $\mathcal{H}_2$ : Hilbert space of the second qubit) is given by:

$$|\uparrow\rangle^{(2)} = \begin{pmatrix} 1 \\ 0 \end{pmatrix} \text{ and } |\downarrow\rangle^{(2)} = \begin{pmatrix} 0 \\ 1 \end{pmatrix}$$

Therefore the basis for the total Hilbert space ( $\mathcal{H}_{tot} = \mathcal{H}_1 \otimes \mathcal{H}_2$ ) is:

$$\mathcal{B}_{\mathcal{H}_{tot}} = \{ |\uparrow\rangle^{(1)} \otimes |\uparrow\rangle^{(2)}, |\uparrow\rangle^{(1)} \otimes |\downarrow\rangle^{(2)}, |\downarrow\rangle^{(1)} \otimes |\uparrow\rangle^{(2)}, |\downarrow\rangle^{(1)} \otimes |\downarrow\rangle^{(2)} \}$$

To simplify the notation in this report, we will use a classical notation:

$$\mathcal{B}_{\mathcal{H}_{tot}} = \{ |\uparrow\uparrow\rangle, |\uparrow\downarrow\rangle, |\downarrow\uparrow\rangle, |\downarrow\downarrow\rangle \} \quad (17)$$

The Hilbert space, a fundamental construct in quantum mechanics and quantum computing, represents the complete set of possible states for a quantum system. However, the vastness of this space often poses significant computational challenges. The reduction of Hilbert space, therefore, becomes a crucial technique for making quantum computations tractable. This process involves identifying and isolating a subspace of the Hilbert space that captures the essential dynamics and properties of the system under consideration.

### B.0.1 Hilbert space reduction

To reduce of the Hilbert space. Let see the action of the  $\hat{\mathcal{H}}$  on the initial state

$$\hat{\mathcal{H}} |\uparrow\downarrow\rangle = \hbar [J + iD(\gamma - 1)] |\downarrow\uparrow\rangle - +\hbar g (|\uparrow\downarrow\rangle - |\uparrow\downarrow\rangle) \quad (18)$$

With [Equation 18](#) the minimal basis of the system is :

$$\mathcal{B}_{red} = \{ |\uparrow\downarrow\rangle, |\downarrow\uparrow\rangle \} \quad (19)$$

So let expressed the Hamiltionian in  $\mathcal{B}_{red}$ , for that let see the action of  $\hat{\mathcal{H}}$  on the  $|\downarrow\uparrow\rangle$

$$\hat{\mathcal{H}} |\downarrow\uparrow\rangle = \hbar [J - iD(\gamma - 1)] |\uparrow\downarrow\rangle - \hbar g (|\downarrow\uparrow\rangle - |\downarrow\uparrow\rangle) \quad (20)$$

So with the the effectif Hamiltionian in  $\mathcal{B}_{red}$  is :

$$\boxed{\hat{\mathcal{H}}_{eff} = \hbar \begin{bmatrix} 0 & \kappa \\ \kappa^* & 0 \end{bmatrix}} \quad (21)$$

where  $\kappa = J + iD(\gamma - 1)$

Let us define  $a = \frac{1+\delta}{2}$  and  $b = \frac{1-\delta}{2}$ , and let us transform the  $\hat{\mathcal{H}}_{XY}$  using [Proposition 4](#):

$$\hat{\mathcal{H}}_{XY} = \hbar J [a (\hat{\sigma}_1^+ + \hat{\sigma}_1^-) (\hat{\sigma}_2^+ + \hat{\sigma}_2^-) - b (\hat{\sigma}_1^+ - \hat{\sigma}_1^-) (\hat{\sigma}_2^+ - \hat{\sigma}_2^-)] + \hbar g \sigma_z^{(1)}$$

Now, let us use the bilinearity and associativity of the Kronecker product:

$$\begin{aligned} \hat{\mathcal{H}}_{XY} = \hbar J & [a (\hat{\sigma}_1^+ \hat{\sigma}_2^+ + \hat{\sigma}_1^+ \hat{\sigma}_2^- + \hat{\sigma}_1^- \hat{\sigma}_2^+ + \hat{\sigma}_1^- \hat{\sigma}_2^-) \\ & - b (\hat{\sigma}_1^+ \hat{\sigma}_2^+ - \hat{\sigma}_1^+ \hat{\sigma}_2^- - \hat{\sigma}_1^- \hat{\sigma}_2^+ + \hat{\sigma}_1^- \hat{\sigma}_2^-)] + \hbar g [\hat{\sigma}_1^z + \hat{\sigma}_2^z] \end{aligned}$$

Since  $a + b = 1$  and  $a - b = \delta$ , we have:

$$\hat{\mathcal{H}}_{XY} = \hbar J [\delta (\hat{\sigma}_1^+ \hat{\sigma}_2^+ + \hat{\sigma}_1^- \hat{\sigma}_2^-) + (\hat{\sigma}_1^+ \hat{\sigma}_2^- + \hat{\sigma}_1^- \hat{\sigma}_2^+)] + \hbar g [\hat{\sigma}_1^z + \hat{\sigma}_2^z]$$

Let us now proceed similarly for  $\hat{\mathcal{H}}_D$ :

$$\begin{aligned} \hat{\mathcal{H}}_D &= \hbar D (\hat{\sigma}_1^x \hat{\sigma}_2^y + \gamma \hat{\sigma}_1^y \hat{\sigma}_2^x) \\ &= -i\hbar D [(\hat{\sigma}_1^+ + \hat{\sigma}_1^-) (\hat{\sigma}_2^+ - \hat{\sigma}_2^-) + \gamma (\hat{\sigma}_1^+ - \hat{\sigma}_1^-) (\hat{\sigma}_2^+ + \hat{\sigma}_2^-)] \quad \text{by Proposition 4} \\ &= -i\hbar D [(\hat{\sigma}_1^+ \hat{\sigma}_2^+ - \hat{\sigma}_1^+ \hat{\sigma}_2^- + \hat{\sigma}_1^- \hat{\sigma}_2^+ - \hat{\sigma}_1^- \hat{\sigma}_2^-) + \gamma (\hat{\sigma}_1^+ \hat{\sigma}_2^+ + \hat{\sigma}_1^+ \hat{\sigma}_2^- - \hat{\sigma}_1^- \hat{\sigma}_2^+ - \hat{\sigma}_1^- \hat{\sigma}_2^-)] \\ &= -i\hbar D [(\gamma + 1) \hat{\sigma}_1^+ \hat{\sigma}_2^+ + (\gamma - 1) \hat{\sigma}_1^+ \hat{\sigma}_2^- - (\gamma - 1) \hat{\sigma}_1^- \hat{\sigma}_2^+ - (\gamma + 1) \hat{\sigma}_1^- \hat{\sigma}_2^-] \\ &= i\hbar D [(\gamma + 1) (\hat{\sigma}_1^- \hat{\sigma}_2^- - \hat{\sigma}_1^+ \hat{\sigma}_2^+) + (\gamma - 1) (\hat{\sigma}_1^- \hat{\sigma}_2^+ - \hat{\sigma}_1^+ \hat{\sigma}_2^-)] \end{aligned}$$

Given the initial state  $|\uparrow\downarrow\rangle$ , as discussed in the section on reduction of Hilbert space, we can reduce the basis of the Hilbert space to  $\mathcal{B}_{red}$ . The operators are as follows:

$$\left\{ \begin{array}{l} i(\hat{\sigma}_1^- \hat{\sigma}_2^+ - \hat{\sigma}_1^+ \hat{\sigma}_2^-)|_{\mathcal{B}_{red}} = \sigma_y \\ \hat{\sigma}_1^+ \hat{\sigma}_2^- + \hat{\sigma}_1^- \hat{\sigma}_2^+|_{\mathcal{B}_{red}} = \sigma_x \\ \hat{\sigma}_1^z|_{\mathcal{B}_{red}} = \sigma_z \\ \hat{\sigma}_2^z|_{\mathcal{B}_{red}} = -\sigma_z \\ \hat{\sigma}_1^+ \hat{\sigma}_2^+ + \hat{\sigma}_1^- \hat{\sigma}_2^-|_{\mathcal{B}_{red}} = \hat{\sigma}_1^- \hat{\sigma}_2^- - \hat{\sigma}_1^+ \hat{\sigma}_2^+|_{\mathcal{B}_{red}} = 0 \end{array} \right. \quad (22)$$

$$\hat{\mathcal{H}}_{\text{eff}} = \hbar(J\sigma_x + D(\gamma - 1)\sigma_y + g\sigma_z)$$

Using [Theorem 2](#) and [Equation 21](#), the evolution operator in the basis  $\mathcal{B}_{red}$  is given by:

$$\hat{U}(t, t_0) = e^{-i\hat{\mathcal{H}}_{\text{eff}}t/\hbar} = \cos(\mu t)\hat{\mathbb{I}} - i \sin(\mu t) \left[ \frac{J\sigma_x + D(\gamma - 1)\sigma_y}{\mu} \right] \quad (23)$$

where  $\mu = \sqrt{J^2 + D^2(\gamma - 1)^2}$ .

Thus, using the definition of the time evolution operator and the properties in [Proposition 5](#), we can compute  $|\psi(t)\rangle$ :

$$|\psi(t)\rangle = \cos(\mu t)|\uparrow\downarrow\rangle - i \sin(\mu t) \left[ \frac{J + iD(\gamma - 1)}{\mu} \right] |\downarrow\uparrow\rangle \quad (24)$$

### Theorem 3: Concurrence of two qubit

Consider a two-qubit system with the basis states  $\mathcal{B} = \{|\downarrow\downarrow\rangle, |\downarrow\uparrow\rangle, |\uparrow\downarrow\rangle, |\uparrow\uparrow\rangle\}$  for its Hilbert space.

For a quantum state  $|\psi\rangle$  in  $\mathcal{B}$  expressed as

$$|\psi\rangle = C_0 |\downarrow\downarrow\rangle + C_1 |\downarrow\uparrow\rangle + C_2 |\uparrow\downarrow\rangle + C_3 |\uparrow\uparrow\rangle \quad (25)$$

where  $\forall i \in [[0, 3]]$ ,  $C_i \in \mathbb{C}$  the concurrence  $C(|\psi\rangle)$  is given by

$$C(|\psi\rangle) = 2 |C_1 C_2 - C_0 C_3| \quad (26)$$

*Proof.* We start by recalling the definition of concurrence  $C(|\psi\rangle)$  for a two-qubit quantum state  $|\psi\rangle$  [10]:

$$C(|\psi\rangle) = |\langle\psi|\sigma_y \otimes \sigma_y|\psi^*\rangle| \quad (27)$$

The action of the tensor product  $\sigma_y \otimes \sigma_y$  on  $|\psi^*\rangle$ , considering the transformation properties of  $\sigma_y$  on the basis states, is computed as:

$$\sigma_y \otimes \sigma_y |\psi^*\rangle = C_0^* |\uparrow\uparrow\rangle + C_1^* |\uparrow\downarrow\rangle + C_2^* |\downarrow\uparrow\rangle + C_3^* |\downarrow\downarrow\rangle \quad (28)$$

Next, we evaluate the inner product  $\langle\psi| \sigma_y \otimes \sigma_y |\psi^*\rangle$ . Recall that the basis states are orthogonal and normalized. Therefore, we only consider terms where the bra and ket vectors match, which gives:

$$\langle\psi| \sigma_y \otimes \sigma_y |\psi\rangle^* = -2C_0C_3 + 2C_1C_2 \quad (29)$$

Thus, the concurrence  $C(|\psi\rangle)$  becomes:

$$C(|\psi\rangle) = 2 |C_1C_2 - C_0C_3|$$

□

So

$$\begin{aligned} C(|\psi(t)\rangle) &= 2 \left| -\cos(\mu t) i \sin(\mu t) \left[ \frac{J + iD(\gamma - 1)}{\mu} \right] \right| \\ &= |\sin(2\mu t)| \end{aligned}$$

$$C(|\psi(t)\rangle) = |\sin(2\mu t)|$$

## C. Appendix C

### Definition 5: Pauli matrices

The Pauli matrices are a set of three  $2 \times 2$  complex matrices which are Hermitian and unitary. They are commonly denoted as  $\hat{\sigma}^x$ ,  $\hat{\sigma}^y$ , and  $\sigma_z$  and are given by:

$$\hat{\sigma}^x = \begin{pmatrix} 0 & 1 \\ 1 & 0 \end{pmatrix}, \quad \hat{\sigma}^y = \begin{pmatrix} 0 & -i \\ i & 0 \end{pmatrix}, \quad \hat{\sigma}^z = \begin{pmatrix} 1 & 0 \\ 0 & -1 \end{pmatrix} \quad \hat{\sigma}^- = \begin{pmatrix} 0 & 0 \\ 1 & 0 \end{pmatrix}, \quad \hat{\sigma}^+ = \begin{pmatrix} 0 & 1 \\ 0 & 0 \end{pmatrix}$$

### Proposition 3: Pauli Matrix

$$\hat{\sigma}^x = \hat{\sigma}^+ + \hat{\sigma}^-, \quad \hat{\sigma}^y = i(\hat{\sigma}^- - \hat{\sigma}^+), \quad \hat{\sigma}^- = \frac{\hat{\sigma}^x - i\hat{\sigma}^y}{2}, \quad \hat{\sigma}^+ = \frac{\hat{\sigma}^x + i\hat{\sigma}^y}{2}$$

*Proof.* Use the [Definition 5](#)

### Proposition 4: Identity Pauli Matrix

$$\hat{\sigma}^y = i\hat{\sigma}^x\hat{\sigma}^z$$

*Proof.* Use the [Definition 5](#)

### Proposition 5: Action of Pauli matrices on spin states

- $\sigma_x$  flips the spin:

$$\sigma_x |\uparrow\rangle = |\downarrow\rangle, \quad \sigma_x |\downarrow\rangle = |\uparrow\rangle$$

- $\sigma_y$  introduces a phase factor  $i$  or  $-i$  and flips the spin:

$$\sigma_y |\uparrow\rangle = i |\downarrow\rangle, \quad \sigma_y |\downarrow\rangle = -i |\uparrow\rangle$$

- $\sigma_z$  leaves the spin-up state unchanged and flips the sign of the spin-down state:

$$\sigma_z |\uparrow\rangle = |\uparrow\rangle, \quad \sigma_z |\downarrow\rangle = - |\downarrow\rangle$$

where  $|\uparrow\rangle = \begin{pmatrix} 1 \\ 0 \end{pmatrix}$  and  $|\downarrow\rangle = \begin{pmatrix} 0 \\ 1 \end{pmatrix}$